

Alkali Metal Complexes of Silyl-Substituted *ansa*-(Tris)allyl Ligands: Metal-, Co-Ligand- and Substituent-Dependent Stereochemistry

Scott A. Sulway,^[a] Roman Girshfeld,^[a] Sophia A. Solomon,^[a] Christopher A. Muryn,^[a] Jordi Poater,^[b] Miquel Solà,^[b] F. Matthias Bickelhaupt,^{*[c]} and Richard A. Layfield^{*[a]}

Keywords: Allyl ligands / Lithium / Sodium / Potassium / Stereochemistry

The structures of alkali metal complexes of silyl-substituted *ansa*-tris(allyl) ligands $[\text{RSi}(\text{C}_3\text{H}_3\text{SiMe}_3)_3]^{3-}$ (R = Me, **L**¹; or Ph, **L**²) are discussed. Triple deprotonation of **L**¹H₃ by *n*BuNa/tmeda affords $[\text{L}^1\{\text{Na}(\text{tmeda})\}_3]$ (**4**) in which the sodium cations are complexed by η^n -allyl ligands and the silyl substituents adopt $[\text{exo},\text{exo}][\text{endo},\text{exo}]_2$ stereochemistries in one crystallographically disordered form and $[\text{endo},\text{exo}]_3$ in another. Triple deprotonation of **L**²H₃ with *n*BuLi/tmeda results in the formation of $[\text{L}^2\{\text{Li}(\text{tmeda})\}_3]$ (**5**), the structure of which features silyl substituents with $[\text{exo},\text{exo}]_2[\text{endo},\text{exo}]$ stereochemistries. The trisodium complex $[\text{L}^2\{\text{Na}(\text{tmeda})\}_2]$ (**6**) consists of a hexa(allylsodium) macrocycle that aggregates as a result of cation- π interactions between the phenyl substituents and the sodium cations. An attempt to prepare the tripotassium complex of **L**¹ resulted in the formation of the bimetallic potassium/lithium complex

$[\text{L}^1\{\text{K}(\text{OEt}_2)_2\}_2\text{KLi}(\mu_4\text{-OtBu})]_2$ (**7**), in which the lithium *tert*-butoxide by-product is incorporated into a hexa(allylpotassium) macrocycle. Triple deprotonation of **L**¹H₃ with *n*BuLi and the terdentate Lewis base pmdeta results in $[\text{L}^1\text{Li}(\text{pmdeta})]_3$ (**8**), in which the three allyl groups do not μ -bridge between lithium cations, resulting in an $[\text{exo},\text{exo}]_3$ stereochemistry of the silyl substituents. NMR spectroscopic studies reveal complicated solution-phase behaviour for **4**, **6** and **7**, whereas the solid-state structures of **5** and **8** are preserved in solution. Further insight into the structures and stereochemical preference of the *ansa*-tris(allyl) ligands in **4** and **5** is provided by detailed density functional theory calculations.

(© Wiley-VCH Verlag GmbH & Co. KGaA, 69451 Weinheim, Germany, 2009)

Introduction

The chemistry of silyl-substituted allyl compounds is extremely diverse. In organic synthesis, allylsilanes are valuable reagents due to the variety of ways in which they can be readily functionalized with electrophiles and radicals.^[1] Conversion of allylsilanes into their corresponding anions is also facile, and the ensuing allylic organometallics are widely employed as carbon nucleophiles.^[2] In a coordination chemistry setting, despite their widespread use in catalysis, allyl complexes of transition metals are notorious for their thermal instability and air-sensitivity.^[3] In contrast, silyl-substituted allyl ligands have allowed access to a broad

range of kinetically stabilized, isolable allyl complexes of *d*-,^[4–12] *f*-^[13–20] and *p*-block,^[21,22] metals. Whereas structural characterization of metal allyl compounds featuring allyl ligands with low steric demands has been rare, in many cases it has been possible to structurally characterize silyl-substituted metal allyl complexes by X-ray crystallography.

The structures of alkali^[23–31] and alkaline earth,^[32,33] metal silylallyls have also been studied in detail. The first such compound to be characterised was *exo,exo*-[1,3-bis(trimethylsilyl)allyllithium] as the tmeda complex $[\text{Li}\{\text{C}_3\text{H}_3\text{-1,3-(SiMe}_3)_2\}(\text{tmeda})]$ (**1**) (tmeda = *N,N,N',N'*-tetramethylethylenediamine). Structural studies on **1** and on other intermolecularly solvated silyl-substituted allyllithium compounds revealed both a preference for *exo* orientations of the silyl substituents with respect to the allyl carbon atoms, and that the allyl ligands tend to coordinate to the lithium cations in an unsymmetrical η^3 -manner. Structural studies on intermolecularly solvated potassium silylallyls have revealed that these compounds tend to exist as zigzag coordination polymers or oligomers in which the allyl ligands adopt $\mu\text{-}\eta^3\text{-}\eta^3$ -coordination modes, with incorporation of solvent molecules such as thf completing the metal coordination environment.^[14,15,34] The polymeric nature of allyl-potassium compounds is a consequence of the larger ionic radius of the cation, which also seems to enable more un-

[a] School of Chemistry, The University of Manchester, Oxford Road, Manchester, M13 9PL, United Kingdom
Fax: +44-161-275-4598
E-mail: Richard.Layfield@manchester.ac.uk

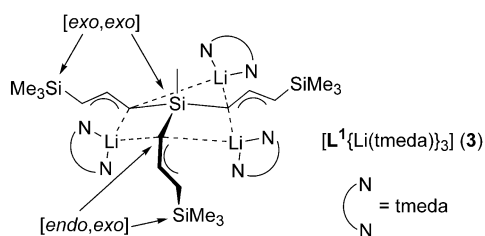
[b] Institut de Química Computacional and Department de Química, Universitat de Girona, 17071 Girona, Catalonia, Spain

[c] Department of Theoretical Chemistry and Amsterdam Center for Multiscale Modeling, Scheikundig Laboratorium der Vrije Universiteit, De Boelelaan 1083, 1081 HV Amsterdam, The Netherlands
Fax: +31-20-5987-629
E-mail: FM.Bickelhaupt@few.vu.nl

Supporting information for this article is available on the WWW under <http://dx.doi.org/10.1002/ejic.200900618>.

symmetrical bonding of the allyl ligand, as witnessed by potassium-carbon bond lengths to the terminal allyl carbon atoms that differ by greater than 0.2 Å in some instances.^[34]

Complexes of *ansa*-bis(silylallyl) ligands, $[\text{Me}_2\text{Si}(\text{C}_3\text{H}_3\text{SiR}_3)_2]^{2-}$ (R_3Si = various silyl groups), with main group and transition metals are also well known.^[28,29] The individual allylmetal units within alkali metal *ansa*-bis(silylallyl) complexes, such as $[\text{Me}_2\text{Si}(\text{C}_3\text{H}_3\text{SiMe}_3)\text{Li}(\text{tmeda})]_2$ (**2**), do not interact with each other via μ -bridging interactions, and are structurally similar to their monoallyl counterparts such as **1**. Recently, the first example of an *ansa*-tris(allyl) complex, $[\text{MeSi}\{\text{C}_3\text{H}_3\text{SiMe}_3\}\text{Li}(\text{tmeda})]_3$, $[\text{L}^1\{\text{Li}(\text{tmeda})\}_3]$ (**3**) ($\text{L}^1 = [\text{MeSi}(\text{C}_3\text{H}_3\text{SiMe}_3)_3]^{3-}$), was reported.^[21] The structure of **3** (see Scheme 1) is different to its mono-allyl and *ansa*-bis(allyl) relatives. Whereas the silyl substituents in lithium mono- and *ansa*-bis(allyl) complexes invariably adopt an *exo* stereochemistry, the three pairs of silyl substituents in **3** (i.e. each of the terminal SiMe_3 groups paired with the central MeSi group) are [*exo,exo*] in two allyllithium units, whereas an [*endo,exo*] stereochemistry is observed in the third, due to a steric interplay between the SiMe_3 substituents, the tmeda co-ligands, and the coordination requirements of lithium. This arrangement of silyl substituents is observed in the solid-state and in benzene solution, and **3** therefore provides the first structurally characterized example of an *endo* silyl substituent in an allyllithium. Secondly, since allyl ligands typically η^3 -coordinate to lithium cations in externally solvated allyls such as **1** and **2**, compound **3** is distinctive for the asymmetric η^2 -bonding of the [*endo,exo*] allyl ligand and the η^1 -bonding of the [*exo,exo*] allyl ligands. In **1** and **2**, each lithium cation is four-coordinate by virtue of a formally bidentate η^3 -allyl ligand and one tmeda ligand; in **3**, the lithium atoms are four-coordinate due to bidentate tmeda ligands and unusual, $\mu:\eta^n$ ($n = 1$ or 2) allyl bonding, which arises from a combination of the pseudo-3-fold symmetry of the *ansa*-tris(allyl) ligand and the small ionic radius of the lithium cations.



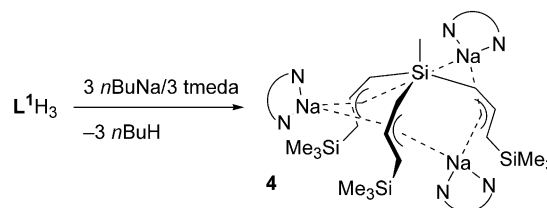
Scheme 1. The *ansa*-tris(allyllithium) **3**.

The unusual structure of **3** has prompted us to undertake more detailed studies of alkali-metal complexes of *ansa*-tris(allyl) ligands. Herein we report the structures of a range of new *ansa*-tris(allyl) complexes of lithium, sodium and potassium; in addition to studying the effect of different alkali metals on *ansa*-tris(allyl) ligand structure, the impact of different co-solvents and *ansa*-tris(allyl) ligand substituents is also explored. Further insight into the observed structural patterns in alkali-metal *ansa*-tris(allyl) complexes is pro-

vided by a computational study of the structures and relative energies of the pristine, trianionic ligand $[\text{L}^1]^{3-}$, and its lithium and sodium complexes.

Results and Discussion

In order to explore the effect(s) that alkali-metal cations of larger radii might have on *ansa*-tris(allyl) ligand structure, the trisodium complex of L^1 was prepared by the addition of the pro-ligand L^1H_3 to a suspension of three equivalents of *n*BuNa in hexane solvent, followed by the addition of one equivalent of tmeda per sodium. The resulting bright orange solution was filtered and stored at -15°C , giving a crop of orange crystals that were subsequently identified by X-ray crystallography to be $[\text{MeSi}\{\text{C}_3\text{H}_3\text{SiMe}_3\}\text{Na}(\text{tmeda})]_3$, $[\text{L}^1\{\text{Na}(\text{tmeda})\}_3]$ (**4**) (Scheme 2 and Figure 1).



Scheme 2. Synthesis of the tmeda-solvated *ansa*-tris(allylsodium) **4**.

Of the three allyl ligand groups in **4**, those containing C(2)–C(3)–C(4) and C(14)–C(15)–C(16) have their silyl substituents in the [*endo,exo*] conformation. The third allyl ligand group, containing C(8)–C(9)–C(10), experiences disorder over two sites, resulting in 51:49 [*endo,exo*]:[*exo,exo*] occupancies. The allyl ligands C(2)–C(3)–C(4) and C(14)–C(15)–C(16) in **4** adopt a $\mu:\eta^3:\eta^3$ bridging mode between Na(2) and Na(3), whereas allyl ligand C(8)–C(9)–C(10) adopts an asymmetric $\mu:\eta^2:\eta^3$ bridging mode between Na(1) and Na(3), which is an unusual bonding mode for an allyl ligand complex of an alkali metal. The range of Na–C bond lengths is 2.553(17)–3.016(12) for Na(1), 2.587(7)–3.193(7) for Na(2) and 2.575(7)–2.882(7) for Na(3). The maximum Na–C bond length recorded in the Cambridge Structural Database is currently 3.199 Å,^[35] which is significantly shorter than the calculated distances of 3.378 and 3.735 Å for Na(1)–C(16) and Na(3)–C(10), respectively. The Na(3)–C(10) distance is too long to be regarded as a sodium-allyl η -type interaction, although the Na(1)–C(16) distance indicates that a weak interaction may be present. Thus, since each sodium is additionally complexed by one bidentate tmeda ligand, the coordination numbers of Na(1), Na(2) and Na(3) are 6, 6 and 5, respectively. The higher coordination numbers of the sodium cations in compound **4**, relative to coordination numbers of 4 for the lithium cations in compound **3**, arise as a result of the greater ionic radius of Na^+ . The asymmetric nature of the μ -allyl coordination modes in **4** is a consequence of the pseudo-3-fold symmetry element in the $[\text{L}^1]^{3-}$ ligand, which results in the Na^+ cations competing for the electron density of the allylic anions. One consequence of the larger ionic radius of so-

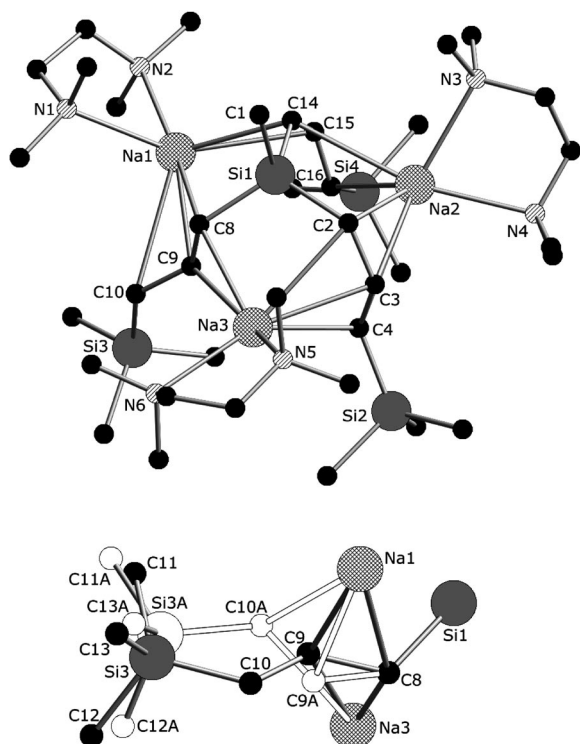


Figure 1. Molecular structure of the $[endo,exo]_2[exo,exo]$ conformation of **4** (upper) and the disordered allylsodium environment of the $[endo,exo]_3$ counterpart (lower). Hydrogen atoms are omitted for clarity. Selected bond lengths [Å] and angles [°] for the $[endo,exo]_2[exo,exo]$ conformation: Si(1)–C(2) 1.874(6), Si(1)–C(8) 1.847(7), Si(1)–C(14) 1.864(7), Na(1)–C(8) 2.718(7), Na(1)–C(9) 2.553(17), Na(1)–C(10) 3.016(12), Na(1)–C(14) 2.614(8), Na(1)–C(15) 2.856(7), Na(2)–C(14) 2.819(7), Na(2)–C(15) 2.652(7), Na(2)–C(16) 2.605(8), Na(2)–C(2) 2.587(7), Na(2)–C(3) 2.762(7), Na(3)–C(2) 2.882(7), Na(3)–C(3) 2.689(7), Na(3)–C(4) 2.677(7), Na(3)–C(8) 2.575(7), Na(3)–C(9) 2.837(16), Na(1)–N(1) 2.501(6), Na(1)–N(2) 2.485(6), Na(2)–N(3) 2.500(6), Na(2)–N(4) 2.500(6), Na(3)–N(5) 2.505(6), Na(3)–N(6) 2.549(6), C(2)–C(3) 1.395(9), C(3)–C(4) 1.368(10), C(8)–C(9) 1.463(13), C(9)–C(10) 1.383(13), C(14)–C(15) 1.391(9), C(15)–C(16) 1.344(9), C(2)–C(3)–C(4) 132.3(7), C(8)–C(9)–C(10) 132.4(12), C(14)–C(15)–C(16) 132.9(8), N(1)–Na(1)–N(2) 72.98(19), N(3)–Na(2)–N(4) 73.63(19), N(5)–Na(3)–N(6) 73.2(2), Na(1)–C(9)–Na(3) 140.8(4), Na(1)–C(15)–Na(2) 129.6(3), Na(2)–C(3)–Na(3) 130.5(3). Selected bond lengths [Å] and angles [°] for the $[endo,exo]_3$ conformation: Na(1)–C(9A) 2.655(18), Na(1)–C(10A) 2.615(13), C(8)–C(9A) 1.394(13), C(9A)–C(10A) 1.365(14), C(8)–C(9A)–C(10A) 123.4(12).

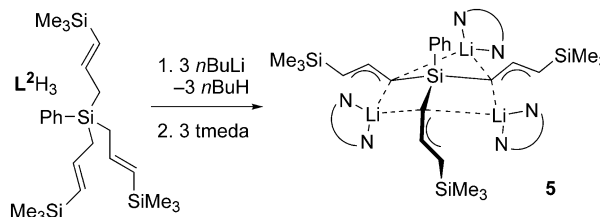
dium is, therefore, to force the three individual silylallyl units to be oriented in the same direction, in contrast to the silylallyl groups in **3** (and compound **5**, see below), which are clearly oriented “away” from each other.

The ^1H NMR spectrum of **4** was recorded in $[\text{D}_6]$ benzene and features resonances arising from the trimethyl and methylsilyl substituents at -0.01 , 0.00 , 0.13 and 0.15 ppm, and broad singlets due to the tmeda co-ligands at $\delta = 2.14$ and 1.95 ppm. The allylic protons occur as several complex, overlapping multiplets (see Supporting Information). The allyl proton resonances in the region $\delta(^1\text{H}) = 5.64$ – 6.46 ppm are mutually coupled, and are also coupled to the proton resonances at $\delta(^1\text{H}) = 1.63$ – 1.86 ppm (which are partially obscured by the resonances due to the tmeda ligands). A

second group of broad, mutually coupled resonances due to allyl protons is observed at $\delta(^1\text{H}) = 2.99$, 3.63 , and 7.35 ppm. These observations point towards the presence of several species in solution at 292.4 K (the temperature at which the spectra were recorded) in benzene. The different forms are likely to correspond to different combinations of *endo* and *exo* stereochemistries of the silylallyl groups, and it is also possible that different orientations of the silylallyl arms in relation to the tmeda co-ligands also contribute to the NMR spectra of **4**.

Structural studies on sodium allyl compounds are rare in comparison to their lithium and potassium analogues. The η^3 -allylsodium coordination in **4** is similar to the η^3 -bonding of the allyl carbon atoms to sodium in the allylbenzene complex $[(\eta^3\text{-C}_3\text{H}_4\text{Ph})\text{Na}(\text{pmdeta})]$ (pmdeta = *N,N,N',N'',N'''*-pentamethyldiethylenetriamine), which also shows highly asymmetric coordination of the allyl carbon atoms with Na–C distances of $2.791(9)$, $2.577(7)$ and $2.676(3)$ Å.^[36] The bimetallic sodium tris(allyl)zincate $[\text{Zn}\{(1,3\text{-Me}_3\text{Si})_2\text{C}_3\text{H}_3\}\text{Na}]$ is also related to **4**, and is a contact ion-pair in which three allyl ligands form σ -bonds to zinc and the localized allyl double bonds coordinate to the sodium cation by means of η^2 -, or cation- π , type interactions.^[10]

In order to explore the impact of varying the substituent on the central silicon atom in *ansa*-tris(allyl) ligands on the structures of their corresponding alkali-metal complexes, the new pro-ligand $[\text{PhSi}(\text{C}_3\text{H}_4\text{SiMe}_3)_3]$ (L^2H_3) was synthesized (see Exp. Sect.). Trilithiation of L^2H_3 with *n*BuLi in hexane/tmeda resulted in the formation of $[\text{PhSi}\{(1,3\text{-Me}_3\text{Si})\text{Li}(\text{tmeda})\}_3]$, $[\text{L}^2\{\text{Li}(\text{tmeda})\}_3]$ (**5**), the structure of which is essentially identical to that of **3**,^[21] featuring three four-coordinate lithium atoms and silyl groups with $[exo,exo]_2[endo,exo]$ conformations (Scheme 3). The pertinent bond lengths and angles in **5** are, unsurprisingly, very similar to those in compound **3**, and so will not be discussed in detail (see Figure 2). The ^1H and ^{13}C NMR spectra of **5** also confirm that the $[exo,exo]_2[endo,exo]$ stereochemistry of the silyl groups is preserved in benzene solution at room temperature.



Scheme 3. Synthesis of the tmeda-solvated *ansa*-tris(allyllithium) **5** showing the $[exo,exo]_2[endo,exo]$ stereochemistry of the silyl groups.

Although replacement of the methyl substituent on the central silicon atom in L^1 with phenyl to give L^2 does not produce marked structural differences between the corresponding trilithium complexes **3** and **5**, the outcome of the reaction of L^2H_3 with benzyllithium, BnNa , was, however, very different. Thus, deprotonation of L^2H_3 with BnNa /tmeda in hexane followed by storage of the concentrated

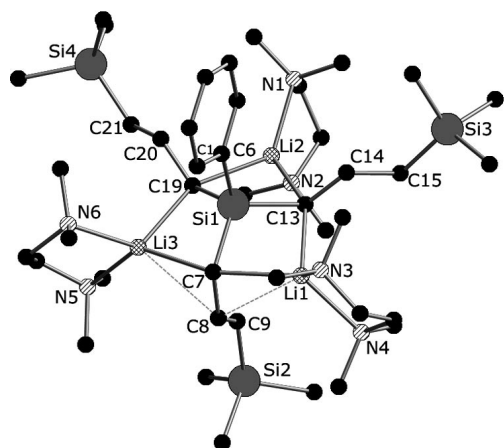
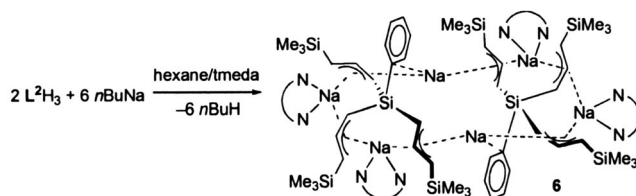


Figure 2. Molecular structure of **5**. Hydrogen atoms are omitted for clarity. Selected bond lengths [Å] and angles [°]: Si(1)–C(7) 1.870(3), Si(1)–C(13) 1.849(2), Si(1)–C(19) 1.852(3), Li(1)–C(7) 2.275(5), Li(1)–C(13) 2.301(5), Li(1)–N(3) 2.164(5), Li(1)–N(4) 2.082(5), Li(2)–C(13) 2.313(5), Li(2)–C(19) 2.250(5), Li(2)–N(1) 2.102(5), Li(2)–N(2) 2.084(5), Li(3)–C(19) 2.267(5), Li(3)–C(7) 2.259(5), Li(3)–N(5) 2.087(6), Li(3)–N(6) 2.147(6), C(7)–C(8) 1.428(4), C(8)–C(9) 1.377(4), C(13)–C(14) 1.418(3), C(14)–C(15) 1.379(3), C(19)–C(20) 1.424(3), C(20)–C(21) 1.377(4), C(7)–C(8)–C(9) 129.5(2), C(13)–C(14)–C(15) 130.7(2), C(19)–C(20)–C(21) 130.5(2), C(7)–Li(1)–C(13) 83.33(17), C(7)–Li(1)–N(3) 114.3(2), C(7)–Li(1)–N(4) 136.9(2), C(13)–Li(1)–N(3) 123.2(2), C(13)–Li(1)–N(4) 118.2(2), N(3)–Li(1)–N(4) 85.91(19), C(13)–Li(2)–C(19) 84.63(16), C(13)–Li(2)–N(1) 127.4(2), C(13)–Li(2)–N(2) 116.1(2), C(19)–Li(2)–N(1) 129.3(2), C(19)–Li(2)–N(2) 113.2(2), N(1)–Li(2)–N(2) 88.61(18), C(7)–Li(3)–C(19) 83.94(18), C(19)–Li(3)–N(5) 115.8(2), C(19)–Li(3)–N(6) 121.2(3), C(7)–Li(3)–N(5) 133.1(3), C(7)–Li(3)–N(6) 120.8(3), N(5)–Li(3)–N(6) 86.4(2).

solution at $-15\text{ }^{\circ}\text{C}$ resulted in the formation of yellow-orange crystals of **6**₂, in which two [PhSi{(C₃H₃SiMe₃)₃Na₃] moieties combine to give a hexametallc macrocycle, with two sodium cations each additionally complexed by a tmeda ligand (Scheme 4). Single crystals of **6**₂ diffracted X-rays weakly, and so the molecular structure was determined using diffraction data from a synchrotron X-ray source (Figure 3). Complex **6**₂ is a centrosymmetric dimer, the monomers of which consist of an [L²]³⁻ ligand bonded to three sodium cations through the allyl carbon atoms in a $\mu\text{:}\eta^3$ manner. The Na–C(allyl) distances fall within the broad range of 2.549(4)–3.472(6) Å (average 2.852 Å), which are typical of the Na–C distances found in sodium complexes of π -bonded organo ligands.^[10,35] Na(1) and Na(3), and symmetry equivalents, are also complexed by one tmeda ligand with Na–N bond lengths in the range 2.420(5)–2.595(4) Å to result in coordination numbers of 6. The monomer units associate by means of sodium cations Na(2) and its symmetry equivalent, which act as bridges between allyl units of the two L² ligands: the absence of tmeda ligands from the coordination spheres of Na(2) and Na(2A) can be assigned to steric congestion arising from SiMe₃ substituents. An additional interaction in the structure of **6**₂ is between the *ipso* carbon of the phenyl rings, C(1), and Na(2). Cation– π interactions of this type are frequently observed in organosodium complexes containing aromatic rings in sufficiently close proximity to the metal

to engage in η^{π} bonding, and have interaction energies of ca. 25 kcal mol⁻¹.^[37] Indeed, this interaction may well exert a structure-directing influence and be responsible for the dimeric structure of **6**₂, since such an interaction is clearly not possible in the methyl-substituted analogue **4**. The stereochemistry of the silyl substituents in **6** is [*exo,exo*][*endo,exo*]₂, presumably because of a drive to minimize clashes between the SiMe₃ groups of one L² ligand and those on the other L² ligand.



Scheme 4. Synthesis of the dimeric *ansa*-tris(allylsodium) **6**₂.

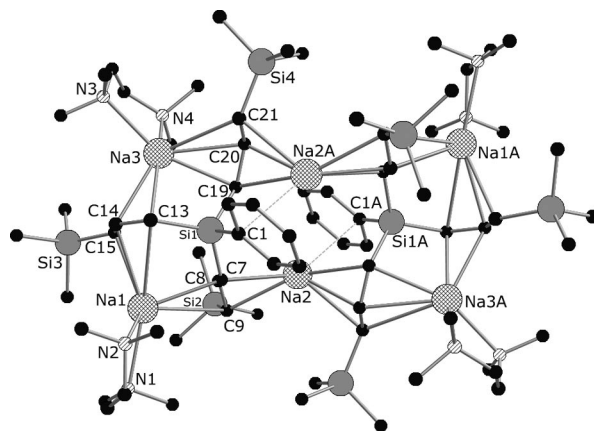
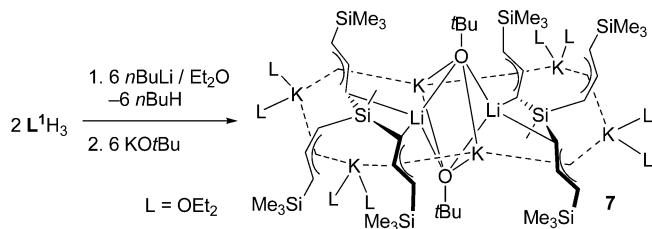


Figure 3. Molecular structure of **6**₂. Hydrogen atoms are omitted for clarity. Selected bond lengths [Å] and angles [°]: Si(1)–C(7) 1.831(3), Si(1)–C(13) 1.863(3), Si(1)–C(19) 1.859(4), Na(2)–C(7) 2.698(4), Na(2)–C(8) 2.831(4), Na(2)–C(9) 2.795(5), Na(2A)–C(19) 2.778(4), Na(2A)–C(20) 2.549(4), Na(2A)–C(21) 2.706(6), Na(2)–C(1A) 2.869(3), C(7)–C(8) 1.415(5), C(8)–C(9) 1.365(6), Na(1)–N(1) 2.595(4), Na(1)–N(2) 2.420(5), Na(1)–C(7) 2.577(3), Na(1)–C(8) 2.831(4), Na(1)–C(9) 3.472(6), Na(1)–C(13) 3.060(4), Na(1)–C(14) 2.768(4), Na(1)–C(15) 2.647(4), C(13)–C(14) 1.391(5), 1.401(5), Na(3)–N(3) 2.442(4), Na(3)–N(4) 2.440(4), Na(3)–C(19) 2.628(4), Na(3)–C(20) 2.733(5), Na(3)–C(21) 3.080(6), C(19)–C(20) 1.379(6), C(20)–C(21) 1.245(8), C(7)–C(8)–C(9) 133.5(4), C(13)–C(14)–C(15) 131.6(3), C(19)–C(20)–C(21) 136.5(5).

Qualitatively, the ¹H NMR spectrum of complex **6**₂ is similar to that of **4**. Thus, in addition to the resonances due to the trimethylsilyl groups, the tmeda co-ligands, and the aromatic protons, the allyl protons occur as two series of complicated overlapping multiplets. The multiplet observed at $\delta(^1\text{H}) = 2.92\text{--}3.81$ ppm was found to couple to two sets of multiplets in the region $\delta(^1\text{H}) = 7.62\text{--}8.40$ ppm. The three, mutually coupled multiplets occurring at $\delta(^1\text{H}) = 5.60\text{--}6.67$ ppm also couple to a multiplet at $\delta(^1\text{H}) = 1.57\text{--}1.73$ ppm, although this signal is partially obscured by the resonances due to the tmeda co-ligands. Given the extent

to which the allyl ^1H resonances in **6**₂ are broadened, conclusions based on integration of the peaks must be made tentatively. However, the similarity of the spectra of **4** and **6**₂ do suggest that the dimeric structure of **6**₂ is intact in benzene solution at room temperature. In the case of **6**₂, the ^1H NMR spectrum indicates that two *ansa*-tris(allylsodium) species are present in solution in an approximate ratio of 3:1 but also that each of these is fluxional in a manner that probably corresponds to *exo*-to-*endo*-to-*exo* interconversions of the trimethylsilyl substituents.

The synthesis of a potassium complex of $[\text{L}^1]^{3-}$ was undertaken by employing a conventional lithiation-transmetalation strategy that involved lithiation of L^1H_3 in diethyl ether followed by addition to potassium *tert*-butoxide. X-ray crystallography revealed that the expected transmetalation of the lithiated ligand by potassium had indeed occurred but also that two equivalents of lithium *tert*-butoxide “by-product” had also been incorporated into the potassium *ansa*-tris(allyl) framework to afford the bimetallic dimer $[\text{L}^1\{\text{K}(\text{OEt}_2)_2\}_2\text{KLi}(\mu_4\text{-O}t\text{Bu})_2, [\mathbf{7}]_2$ (Scheme 5 and Figure 4).



Scheme 5. Synthesis of the bimetallic dimer $[\mathbf{7}]_2$.

The structure of the tripotassium *ansa*-tris(allyl) component of **7** is qualitatively similar to that of the sodium analogue **6**, the main difference being that the silyl substituents in **7** adopt the [*exo*,*exo*]₂[*endo*,*exo*] stereochemistry seen in the structures of **3** and **5**. The K–C(allyl) bonds in **7** also lie within a broad range of 2.921(6)–3.544(6) Å (average 3.118 Å), with K(1) and K(2) and symmetry equivalents each being solvated by two diethyl ether molecules. The two *ansa*-tris(allyl) monomer units of **7** associate by means of K(3) acting as a bridge between η^3 -bonded allyl components of the two $[\text{L}^1]^{3-}$ ligands. In addition, the two bridging potassium atoms bond to the *tert*-butoxide ligands to produce K(3)–O(1) and K(3)–O(1A) bond lengths of 2.829(4) and 2.904(4) Å, respectively. The η^3 -allyl coordination to the potassium cations in **7** is essentially the same as in all structurally characterized silyl-substituted allylpotassium compounds. The lithium *tert*-butoxide core of **7** can be regarded as a trapped $[\text{LiO}t\text{Bu}]_2$ dimer, with the four-coordinate lithium cation Li(1) being complexed by two allylic carbon atoms from an $[\text{L}^1]^{3-}$ ligand, with Li(1)–C(2) and Li(1)–C(14) bond lengths of 2.326(11) and 2.334(10) Å, respectively, and the two oxygens of the *tert*-butoxides with Li(1)–O(1) and Li(1)–O(1A) distances of 1.889(10) and 1.877(10) Å, respectively. The *tert*-butoxide ligands in **7** adopt μ_4 -O*t*Bu bridging modes between K(1/1A) and Li(1/1A) such that the oxygen atoms are five-coordinate at the centre of a distorted trigonal bipyramid. The bimetallic

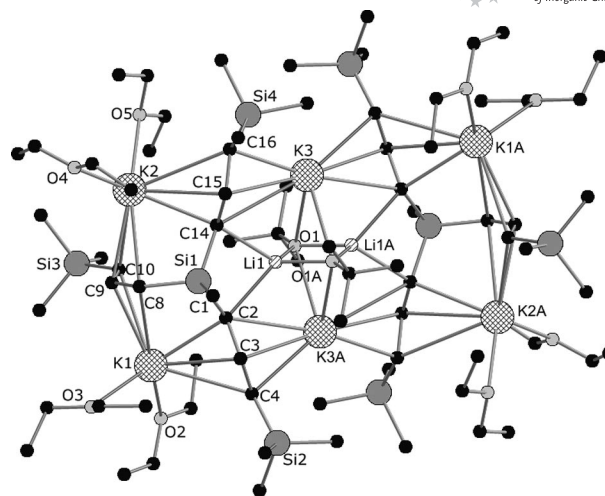


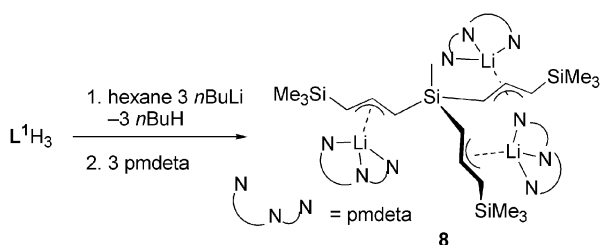
Figure 4. Molecular structure of **7**. Hydrogen atoms are omitted for clarity. Selected bond lengths [Å] and angles [°]: Si(1)–C(2) 1.856(5), Si(1)–C(8) 1.855(6), Si(1)–C(14) 1.853(6), K(1)–C(2) 2.921(6), K(1)–C(3) 3.062(5), K(1)–C(4) 3.308(6), K(1)–C(8) 3.196(6), K(1)–C(9) 3.014(6), K(1)–C(10) 3.157(6), K(2)–C(8) 3.069(6), K(2)–C(9) 2.967(6), K(2)–C(10) 3.090(6), K(2)–C(14) 2.930(6), K(2)–C(15) 3.210(6), K(2)–C(16) 3.544(6), K(3)–C(14) 3.309(6), K(3)–C(15) 3.116(6), K(3)–C(16) 3.003(6), K(3A)–C(2) 3.252(5), K(3A)–C(3) 3.102(5), K(3A)–C(4) 3.005(6), C(2)–C(3) 1.392(8), C(3)–C(4) 1.383(8), C(8)–C(9) 1.363(8), C(9)–C(10) 1.394(8), C(14)–C(15) 1.391(8), C(15)–C(16) 1.397(8), K(1)–O(2) 2.805(4), K(1)–O(3) 2.717(4), K(2)–O(4) 2.726(4), K(2)–O(5) 2.798(5), K(3)–O(1) 2.829(4), K(3)–O(1A) 2.904(4), Li(1)–O(1) 1.889(10), Li(1)–Li(1A) 1.877(10), Li(1)–C(2) 2.326(11), Li(1)–C(14) 2.334(10), O(1)–K(3)–O(1A) 54.93(13), K(3)–O(1)–K(3A) 125.07(13), O(1)–Li(1)–O(1A) 89.3(4), O(1)–Li(1)–C(2) 128.4(5), O(1)–Li(1)–C(14) 128.4(5), C(2)–Li(1)–C(14) 80.3(4), O(1A)–Li(1)–C(2) 116.2(5), O(1A)–Li(1)–C(14) 117.8(5).

core of **7** is reminiscent of the structure of the bimetallic lithium-potassium *tert*-butoxide cage compound $[\text{Li}_4\text{K}_4(\text{O}t\text{Bu})_8]$, in which the O*t*Bu ligands μ_3 - and μ_4 -bridge between the metal ions.^[38] The dimeric $[\text{LiO}t\text{Bu}]_2$ structural motif in **7** is similar to the sub-units found in the structures of the parent compound lithium *tert*-butoxide, which has been found to exist in two structural forms, a hexamer and an octamer. The hexameric cage structure $[\text{LiO}t\text{Bu}]_6$ is thought to occur as a result of the lateral association of $[\text{LiO}t\text{Bu}]_2$ dimers that form the rungs of a cyclic ladder structure. In the unusual, kinetically stable octamer $[\text{LiO}t\text{Bu}]_8$, the same dimers are believed to associate in the first instance to form face-opened tetramers, which themselves combine to form the octamer.^[39]

As with the ^1H NMR spectra of compounds **4** and **6**₂, that of compound **7** is also rather complicated in the allylic region. A series of broad overlapping multiplets at $\delta(^1\text{H}) = 6.41$ – 5.25 ppm coupled with three broadened doublets of doublets at 1.66–1.44 ppm point towards extensive conformational flexibility in benzene at 294.9 K. The sharp, intense singlet for the *tert*-butoxide protons at $\delta(^1\text{H}) = 1.15$ ppm overlaps with the allylic signals in this region, hindering their accurate integration. The complicated solution-phase behaviour of the sodium and potassium allyl compounds **4**, **6** and **7** is in marked contrast to that of the lith-

ium allyl compounds **3** and **5**, which is comparatively straightforward to interpret. That the steric properties of ligand substituents and cation “size” strongly influence the structural properties of alkali-metal compounds is well known. In compounds **4**, **6** and **7**, the relatively large radii of Na^+ and K^+ require higher coordination numbers than the Li^+ cations in **3** and **5**. If the coordination requirements of Na^+ and K^+ have a dominant influence then the silyl substituents and the tmeda or Et_2O co-ligands conceivably are forced into orientations that result in relatively unfavourable steric interactions with other substituents. In solution at room temperature, it is possible that sufficient thermal energy is present to permit fleeting relief of these unfavourable steric interactions by the ligand adopting different conformations, leading to the observed complicated NMR spectra. In compounds **3** and **5**, the coordination requirements of the relatively small Li^+ cations can be satisfied in a manner that orients the silyl substituents away from each other and from the tmeda ligands, resulting in an overall conformation that does not experience steric congestion of the sort observed in **4**, **6**, and **7**.

The influence of the higher denticity co-solvent *N,N,N',N'',N'''*-pentamethyldiethylenetriamine (pmdeta) on *ansa*-tris(allyl) anion structure was investigated by addition of the terdentate Lewis base to a reaction mixture of L^1H_3 and *n*BuLi in hexane. The result was the formation of $[\text{MeSi}\{\text{C}_3\text{H}_3\text{SiMe}_3\}\text{Li}(\text{pmdeta})_3]$ (**8**) as red crystals (Scheme 6 and Figure 5).



Scheme 6. Synthesis of the pmdeata-solvated *ansa*-tris(allyllithium) **8** showing the *[exo,exo]*₃ stereochemistry of the silyl substituents.

Comparing the structure of **8** with those of the lithium complexes **3** and **5** reveals that terdentate coordination of the pmdeata ligands in **8** occurs in preference to μ -allyl bridging mode seen in the tmeda complexes $[\text{RSi}\{\text{C}_3\text{H}_3\text{SiMe}_3\}\text{Li}(\text{tmeda})_3]$. The result is that each allylic ligand in **8** coordinates to a lithium in the more conventional η^3 -mode found in tmeda and pmdeata complexes of silyl-substituted mono-allyllithium compounds and their *ansa*-bis(allyl) analogues,^[23,28,29] resulting in each lithium having a coordination number of 5 in complex **8**. There are two short and one long Li–C distances within each allyllithium group of **8**: the longer Li–C distances of 2.655(10), 2.400(11) and 2.448(11) Å are between Li(1)–C(2), Li(2)–C(17) and Li(3)–C(34), respectively, i.e. the carbon atoms bonded to the central silicon atom Si(1). The Li–C distances to the central and terminal allylic carbon atoms are in the range 2.311(10)–2.377(11) Å (average 2.330 Å). This

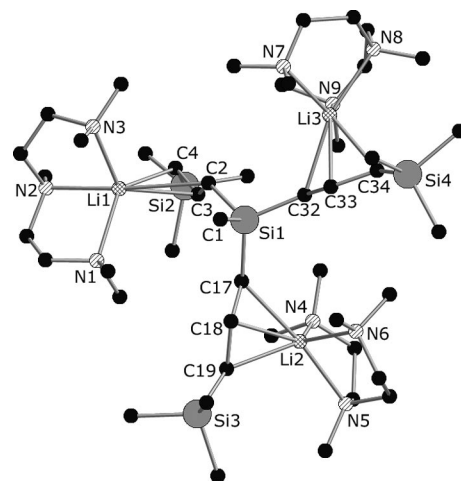


Figure 5. Molecular structure of **8**. Hydrogen atoms are omitted for clarity. Selected bond lengths [Å] and angles [°]: Si(1)–C(2) 1.861(5), Si(1)–C(17) 1.861(5), Si(1)–C(32) 1.852(5), Li(1)–C(2) 2.655(1), Li(1)–C(3) 2.311(10), Li(1)–C(4) 2.315(10), Li(1)–N(1) 2.232(10), Li(1)–N(2) 2.222(10), Li(1)–N(3) 2.220(10), Li(2)–C(17) 2.400(11), Li(2)–C(18) 2.328(11), Li(2)–C(19) 2.316(11), Li(2)–N(4) 2.265(10), Li(2)–N(5) 2.314(10), Li(2)–N(6) 2.141(10), Li(3)–C(32) 2.377(11), Li(3)–C(33) 2.333(11), Li(3)–C(34) 2.448(11), Li(3)–N(7) 2.209(11), Li(3)–N(8) 2.232(11), Li(3)–N(9) 2.306(11), C(2)–C(3)–C(4) 130.9(5), C(17)–C(18)–C(19) 129.5(5), C(32)–C(33)–C(34) 130.8(5).

asymmetry in the η^3 -bonding of the allyl groups to lithium in **8** is also seen in the crystal structure of $[\text{Li}(\text{C}_3\text{H}_5)(\text{pmdeta})]$, in which the Li–C bonds to the terminal allylic carbon atoms differ by almost 0.5 Å at 2.255(5) and 2.720(4) Å, leading to the suggestion that η^2 -allyl coordination is a more accurate description of the bonding mode.^[40] The asymmetric allyl coordination in **8** is likely to arise from steric clashes between the three pmdeata ligands, and may indicate partial delocalization of the formal negative charges within the allyl anions as has previously been observed in intramolecularly solvated alkali-metal allyl compounds.^[24–27,30,41] Indeed, it is notable that the allylic carbon–carbon bonds in **8** are unequal in length, with C(2)–C(3) and C(3)–C(4) being 1.382(7) and 1.426(7) Å, C(17)–C(18) and C(18)–C(19) being 1.367(7) and 1.424(7), and C(32)–C(33) and C(33)–C(34) being 1.379(7) and 1.414(8) Å, respectively. Whereas in the tmeda-solvated complexes **3** and **5** the terminal SiMe_3 and central SiR substituents adopt a mixed *[exo,exo]*₂*[endo,exo]* stereochemistry, the analogous substituents in **8** are *[exo,exo]*₃, the reasons being attributable to the fact that the individual allyllithium units do not influence each other by means of μ -bridging interactions.

The ^1H and ^{13}C NMR spectra of **8**, recorded in $[\text{D}_6]$ -benzene, reveal the presence of three structurally similar, but not identical, allylic $[(\text{pmdeta})\text{Li}(\text{C}_3\text{H}_3\text{SiMe}_3)]$ units. Three unique trimethylsilyl substituents are observed in the ^1H NMR spectrum at $\delta(^1\text{H}) = 0.14, 0.16$ and 0.23 ppm, with the methyl group on the central silicon occurring at $\delta(^1\text{H}) = 0.00$ ppm. The allylic protons occur as a series of overlapping multiplets; the C2 (i.e. central) allylic protons

are observed in the region $\delta(^1\text{H}) = 5.46\text{--}5.76$, $6.08\text{--}6.24$, $6.53\text{--}6.58$ and 7.09 ppm as overlapping multiplets, whereas the terminal allylic protons occur as doublets of doublets at $\delta(^1\text{H}) = 1.61\text{--}1.80$ ppm. In some instances it was possible to measure 3J and 4J coupling constants for the allylic protons; for the former, values of $^3J = 7.78$ and 15.81 Hz suggested the presence of both *endo*- and *exo*-oriented silyl groups. These observations suggest that, in solution, the allylic protons in **8** are in chemically very similar, but not identical, environments. The chemical shifts of the various ^1H environments in the pmdda ligands are similar to those found in other lithium complexes of this ligand.

Computational Studies

In order to study the structures, stereochemical preferences and relative energies of *ansa*-tris(allyl) ligands and their complexes with alkali metals, we have applied density functional theory (DFT), at various levels of theory, to the pristine ligand trianion $[\text{MeSi}\{\text{C}_3\text{H}_3(\text{SiMe}_3)\}_3]^{3-}$, and to complexes **3** and **4**. Calculations on the other complexes discussed in the preceding section were not undertaken due to the excessive amounts of computational time required.

Pristine Trianion $[\text{L}^1]^{3-}$: Irrespective of the level of theory employed, the energetically most favourable stereochemistry of the silyl substituents in the pristine ligand trianion $[\text{MeSi}\{\text{C}_3\text{H}_3(\text{SiMe}_3)\}_3]^{3-}$ is $[\text{exo},\text{exo}]_3$ (Table 1). The results of the calculations also reveal that stability decreases as the number of allyl groups with *endo* stereochemistries with respect to the central SiMe group increases, presumably for steric reasons.

$[\text{L}^1\{\text{Li}(\text{tmeda})\}_3]$ (3**):** A change in the energetically preferred structure occurs upon coordination of the pristine $[\text{L}^1]^{3-}$ anion to three $[\text{Li}(\text{tmeda})]^+$ cations from $[\text{exo},\text{exo}]_3$ to $[\text{exo},\text{exo}]_2[\text{endo},\text{exo}]$ with the BP86/DZP//BP86/DZP method, in agreement with the experimental structure of complex **3** (Table 1). In all methods used, the $[\text{exo},\text{exo}]_3$ and $[\text{exo},\text{exo}]_2[\text{endo},\text{exo}]$ conformations are essentially equal in energy. At the BP86/DZP//BP86/DZP level of theory the $[\text{exo},\text{exo}]_3$ form is only 0.01 kcal mol $^{-1}$ higher than $[\text{exo},\text{exo}]_2[\text{endo},\text{exo}]$. Computations at other levels of theory (except VWN/DZP//VWN/DZP) slightly favour the $[\text{exo},\text{exo}]_3$ form, revealing that these two configurations are very close in energy. Consequently, it is possible that environment effects may play a role in determining the preference of one stereochemistry over the other. An estimation of the effects of the molecular environment on the relative stabilities of the configurations of **3** was performed by simulating the effect of solvation by water using the COSMO model at the BP86/DZP//VWN/DZP level of theory. Comparing the gas- and condensed-phase energies of **3** in Table 1, solvation has essentially no effect on the relative stabilities. However, the COSMO model considers the environment in an average manner and does not take into account specific interactions, therefore the estimate of environment effects is only a rough one. The key bond lengths for the crystallographically determined and computed structures of **3** reveal good

Table 1. Relative energies, ΔE in kcal mol $^{-1}$, of the structural configurations of the pristine anion $[\text{L}^1]^{3-}$, compound **3** and compound **4**.

$[\text{exo},\text{exo}]_n[\text{endo},\text{exo}]_{3-n}$	$[\text{L}^1]^{3-}$	3 ^[a]	4
VWN/DZP//VWN/DZP			
$n = 3$	0.0	10.6	11.5
$n = 2$	2.8	6.2	4.9
$n = 1$	5.4	6.0	1.4
$n = 0$	7.6	0.0	0.0
BP86/DZP//VWN/DZP			
$n = 3$	0.0	0.0	4.6
$n = 2$	4.2	0.8	0.0
$n = 1$	8.3	7.3	0.8
$n = 0$	11.8	7.6	4.8
BP86/TZ2P//VWN/DZP			
$n = 3$	0.0	0.0	4.8
$n = 2$	4.6	2.0	0.0
$n = 1$	9.1	10.0	3.3
$n = 0$	13.0	11.0	6.8
BP86/DZP//BP86/DZP			
$n = 3$	0.0	0.0	4.8
$n = 2$	3.7	0.0	0.0
$n = 1$	7.3	4.3	1.0
$n = 0$	10.5	5.0	5.0
BP86/TZ2P//BP86/TZ2P			
$n = 3$	[b]	0.0	[b]
$n = 2$	[b]	1.2	[b]
$n = 1$	[b]	[b]	[b]
$n = 0$	[b]	[b]	[b]
COSMO-BP86/TZ2P//VWN/DZP			
$n = 3$	0.0	0.0	1.9
$n = 2$	2.7	2.4	0.0
$n = 1$	5.3	10.5	2.8
$n = 0$	8.1	10.6	7.2

[a] See ref.^[21] [b] Not computed.

agreement between experiment and theory (see Supporting Information, Table S1 and Figure S1). For the coordination environment of the lithium cations in **3**, the VWN-level calculations give more accurate reproductions of the Li–C, Li–N, allyl C–C and C–Si bond lengths, whereas the BP86-level calculations give a better reproduction of the location of the $[\text{Li}(\text{tmeda})]^+$ cations.

$[\text{L}^1\{\text{Na}(\text{tmeda})\}_3]$ (4**):** A distinct preference for the $[\text{exo},\text{exo}]_2[\text{endo},\text{exo}]$ stereochemistry was calculated for complex **4** at all levels of theory except VWN/DZP//VWN/DZP, whereas $[\text{endo},\text{exo}]_3$ was found to be the least stable configuration by $4.8\text{--}6.0$ kcal mol $^{-1}$. The energy of the $[\text{exo},\text{exo}]_3$ conformation of **4** was calculated to be the third highest in energy, and the $[\text{exo},\text{exo}][\text{endo},\text{exo}]_2$ conformation (one of the disordered forms of **4** to be determined crystallographically) the second highest in energy across the levels of theory employed. The relative energies of the $[\text{exo},\text{exo}]_3$ and $[\text{exo},\text{exo}][\text{endo},\text{exo}]_2$ conformations actually invert when solvation effects are introduced in COSMO calculations. These results partly contradict the experimental observations on the crystallographically determined structure of **4**. Whereas the $[\text{exo},\text{exo}][\text{endo},\text{exo}]_2$ conformation is found to be quite close to the lowest energy conformation in accordance with experiment, the $[\text{endo},\text{exo}]_3$ conformation, which should be the most stable form, is found to be higher in energy than the $[\text{exo},\text{exo}]_2[\text{endo},\text{exo}]$ and $[\text{exo},\text{exo}]$ -

[*endo,exo*]₂ conformations, in disagreement with experiment. This contradiction between experiment and theory could conceivably be due to the fact that the model system employed does not take into account factors such as the van der Waals interactions between neighbouring molecules of **4** and the effects of crystallographic disorder. Again, computed geometric parameters are in relatively good agreement with X-ray data (see Supporting Information, Tables S1 and S2). The most important difference is the closer proximity of the C(8) allyl group to Na(1) rather than Na(3), thus deviating from the more symmetrical X-ray structure of **4**. VWN reproduces more accurately the Na–C and Na–N distances, whereas BP86 shows a better reproduction of Si–C and C–C distances.

Stereochemical Considerations: The ease with which allylsilanes can be deprotonated and subsequently functionalized with electrophiles makes them attractive synthetic building blocks. Quenching metallated allylsilanes with electrophiles results in the formation of *Z* or *E* isomers of silylalkenes. Furthermore, in the case of mono- or other unsymmetrically substituted allylsilane anions, the product of electrophile quenching may occur as one of two regioisomers (i.e. the electrophile may add to C1 or C3). In the case of (trimethylsilyl)allyllithium, for example, electrophile quenching produces the corresponding (*E*)-silylalkene with the electrophile having added to the unsubstituted allyl carbon. This observation suggested that the trimethylsilyl substituent adopts an *exo* stereochemistry in the allyllithium intermediate, as it also does in the potassium analogue.^[42]

Methods that permit control over the stereo- and regioselectivities with which allylsilanes react with electrophiles are desirable. Because the *Z* or *E* stereoselectivity in such reactions is believed to be dependent on the *endo* or *exo* position of the trimethylsilyl group in the allylmetal intermediate, to obtain control over stereochemistry it is first of all necessary to influence the structures of the silylallyl ligand component of these intermediates. The *ansa*-tris(allyl) ligands within complexes **3–8** carry silyl substituents that can exist in four possible combinations of [*exo,exo*]_{*n*}[*endo,exo*]_{*3–n*} stereochemistries, and we have shown in this paper that the precise stereochemistry adopted depends on the alkali metal, the substituent on the central silicon atom in the *ansa*-tris(allyl) ligand, and the added co-solvent. Control over this stereochemistry in solution clearly presents a major challenge due to the inherent configurational instability of the allyllithium, -sodium and -potassium compounds described. Building on our current findings, our future work in this area will examine possible methods of exerting the desired control through the use of, for example, chiral co-ligands such as (–)-sparteine. Ultimately, this may allow us to develop new allyl alkali-metal compounds for use in regio- and stereoselective synthesis.

Conclusions

Lithium, sodium, and potassium complexes of the *ansa*-tris(allyl) ligands [L¹]^{3–} and [L²]^{3–} have been synthesized

and crystallographically characterized. The crystal structures of complexes **4–8** have revealed that, in the solid-state, the ionic radius of the alkali metal, the denticity of the co-ligands (such as *tmeda* and *pmdeta*) and, surprisingly, the substituent on the *ansa*-tris(allyl) central silicon atoms can strongly influence the molecular structure of the complex and the stereochemistry of the trimethylsilyl substituents. A theoretical study of complexes **4** and **5** (and of the pristine ligand trianion [L¹]^{3–}) revealed relatively small energy differences between the experimentally observed structures of **4** and **5** and other conformations of these complexes in which the silyl substituents adopt different stereochemistries with respect to the allylic carbon atoms. The small energy differences between various conformations of the *ansa*-tris(allyl) complexes is reflected in their solution-state ¹H and ¹³C NMR spectra, which reveal several species in solution and reflect extensive configurational instability in the structures of **4–8**.

Experimental Section

General: All experimental procedures were performed using standard Schlenk techniques under an inert atmosphere of dinitrogen dried with silica columns or molecular sieves. The pro-ligand L¹H₃ was synthesized according to a literature method,^[21] and all other starting materials were purchased from Sigma–Aldrich. Dried, degassed solvents were obtained from an Innovative Technology Solvent Purification System. X-ray diffraction data on complexes **4** and **6–8** were obtained on an Oxford Instruments XCaliber 2 CCD diffractometer, and data for complex **5** were collected at the Daresbury SRS using synchrotron radiation and a Bruker Apex II CCD diffractometer. NMR spectra were recorded on Bruker Avance 400 or 500 MHz NMR spectrometers.

The reference codes for the crystal structures reported in this paper are CCDC-728544 (for **4**), -728545 (for **5**), -728546 (for **6**), -728542 (for **7**), and -728543 (for **8**). Selected crystal data and structure refinement are presented in Table 2. Full crystallographic data for these compounds can be obtained free of charge from The Cambridge Crystallographic Data Centre via www.ccdc.ac.uk/data_request.cif.

PhSi(C₃H₄SiMe₃)₃, L²H₃: A mixture of allyltrimethylsilane (15.67 g, 137 mmol) and thf (80 mL) was cooled to –78 °C and *n*BuLi (1.4 M, 85.5 mL, 0.137 mmol) was added dropwise over 30 min. The solution was stirred at –78 °C for 30 min and then warmed to room temperature. After 18 h a red/orange solution was obtained, to which trichlorophenylsilane (10.57 g, 50 mmol) was added dropwise over 10 min, at –10 °C. The orange/red colour was discharged and the mixture stirred overnight to result in the formation of a colourless solution and precipitate. The thf solvent was removed in vacuo and replaced with diethyl ether (80 mL). Following filtration of the solution (Celite, P3) and evaporation of the solvent, the resulting pale yellow oil was purified by column chromatography (silica, hexane eluant). The hexane eluent was evaporated to produce a viscous yellow oil (11.76 g, 58%). C₂₄Si₄H₄₄ (444.96): calcd. C 64.86, H 9.90; found C 64.63, H 10.02. ¹H NMR (500.13 MHz, CDCl₃, 294.3 K): δ = 1.90 (s, 21 H, SiMe₃), 5.45 (t, 6 H, CH₂CHCH), 5.50 (d, 3 H, CH₂CHCH), 6.00 (m, 3 H, CH₂CHCH), 7.25 (d, 2 H, *m*-C₆H₅-Si), 7.27 (t, 1 H, *p*-C₆H₅-Si), 7.45 (d, 2 H, *o*-C₆H₅-Si) ppm. ¹³C NMR (125.76 MHz, CDCl₃, 295.8 K): δ = 0.00 (SiMe₃), 23 (PhSi-CH₂), 127 (Me₃Si-

Table 2. Crystallographic details for compounds **4**, **5**, **6**, **7** and **8**.

	4	5	6	7	8
Empirical formula	C ₃₇ H ₈₇ N ₆ Na ₃ Si ₄	C ₄₅ H ₉₆ Li ₃ N ₆ Si ₄	C ₇₂ H ₁₄₆ N ₈ Na ₆ Si ₈	C ₇₈ H ₁₇₆ K ₆ Li ₂ O ₁₀ Si ₈	C ₄₆ H ₁₀₈ Li ₃ N ₉ Si ₄
<i>M_r</i>	797.46	854.56	1486.63	1747.39	920.59
<i>T</i> [K]	100(2)	100(2)	100(2)	100(2)	100(2)
Crystal system	monoclinic	triclinic	monoclinic	monoclinic	triclinic
Space group	<i>P</i> 2 ₁ / <i>n</i>	<i>P</i> $\bar{1}$	<i>P</i> 2 ₁ / <i>n</i>	<i>P</i> 2 ₁ / <i>n</i>	<i>P</i> $\bar{1}$
<i>a</i> [Å]	11.352(5)	12.025(5)	12.8897(8)	10.4657(17)	16.0060(8)
<i>b</i> [Å]	41.690(5)	14.431(5)	15.1365(9)	30.656(4)	16.1880(9)
<i>c</i> [Å]	11.407(5)	18.953(5)	24.2992(14)	17.2525(19)	24.1430(12)
α [°]		78.384(5)			86.404(4)
β [°]	105.088(5)	87.499(5)	94.1500(10)	101.553(13)	86.051(4)
γ [°]		65.960(5)			78.898(5)
<i>V</i> [mm ³]	5212(3)	2939.5(18)	4728.5(5)	5423.1(12)	6116.1(5)
<i>Z</i>	4	2	2	2	4
ρ_{calcd} [Mg m ⁻³]	1.016	0.965	1.044	1.070	1.000
<i>M</i> [mm ⁻¹]	0.168	0.132	0.180	0.373	0.132
θ Range [°]	3.72–23.25	3.71–28.28	3.51–25.00	4.11–25.35	3.74–25.03
Completeness	99.5	96.7	99.1	99.2	99.3
Number of reflections	14309	37261	37930	31107	63988
Unique reflections (<i>R</i> _{int})	7448 (0.0832)	14095 (0.0281)	8876 (0.0545)	9856 (0.0629)	21480 (0.0464)
Data/restraints/parameter	7448/153/519	14096/22/581	8876/12/470	9856/0/523	21480/0/1186
Goodness-of-fit on <i>F</i> ²	1.102	1.067	1.100	1.305	1.114
<i>R</i> ₁ [<i>I</i> > 2 σ (<i>I</i>)]	0.1038	0.0656	0.0867	0.0996	0.0934
<i>wR</i> ₂ (all data)	0.1986	0.221	0.2524	0.1952	0.2451
Largest diff. peak and hole	0.541 and –0.331	1.379 and –0.554	1.408 and –0.770	1.027 and –0.563	0.760 and –0.538

CH=CH-CH₂), 130 (*o*-C₆H₅Si), 135, 138, 139, 143 (*ipso*-C₆H₅Si) ppm. MS ES/CI: *m/z* = 445 [M + Cl]⁺, (331) [loss of one allyl trimethylsilane], 72 [phenyl ring].

[L¹{Na(tmEDA)}₃] (4): A suspension of *n*BuNa, freshly prepared from sodium *tert*-butoxide (0.29 g, 3.0 mmol) and *n*BuLi (1.6 mL, 3.0 mmol), in hexane (20 mL) was cooled to –78 °C and L¹H₃ (0.39 g, 1.0 mmol) was added dropwise over 1 min. The reaction mixture was then slowly warmed to room temperature and stirred for 1 h. On re-cooling to –78 °C, tmEDA (0.35 g, 0.46 mL, 3.0 mmol) was added to the pale yellow reaction mixture, which was stirred for 15 min and then warmed to room temperature. Stirring for 18 h produced a bright orange solution that was filtered (Celite, P3) and concentrated to ca. 4 mL. Storage of the concentrated solution at –15 °C for several days produced large, orange block-like crystals of compound **4** (0.30 g, 38% isolated yield). C₃₇H₈₇N₆Na₃Si₄: calcd. C 55.73, H 11.00, N 10.54; found C 55.01, H 10.25, N 9.98. ¹H NMR (400.23 MHz, [D₆]benzene, 294.3 K): δ = –0.01, 0.00, 0.15, 0.13 (s, 30 H, SiMe₃ and SiMe), 1.63, 1.70, 1.79, 1.86 (overlapping d, allyl H), 1.95 (s, 12 H, tmEDA CH₂), 2.14 (s, 12 H, tmEDA CH₃), 2.99 (br. d, allyl H), 3.63 (br. m, allyl H), 5.64 (overlapping m, allyl H), 6.20 (overlapping m, allyl H), 6.46 (overlapping m, allyl H), 7.35 (br. m, allyl H) ppm. ¹³C NMR (100.65 MHz, [D₆]benzene, 295.8 K): δ = –4.42, –2.27, –1.20, 2.77 (SiMe₃ and SiMe), 27.85 (allyl C), 56.72 (tmEDA CH₂), 45.38 (tmEDA CH₃), 73.38 (allyl C), 76.61 (allyl C), 129.02 (allyl C), 145.68 (allyl C), 151.12 ppm.

[L²{Li(tmEDA)}₃] (5): Complex **5** was prepared in an identical manner to the previously reported complex [L¹{Li(tmEDA)}₃], using L²H₃ (0.51 g, 1.1 mmol), hexane solvent (10 mL), *n*BuLi (1.6 mL, 2.14 mL, 3.4 mmol) and tmEDA (0.51 mL, 0.40 g, 3.4 mmol). Storage of a concentrated solution at +5 °C overnight afforded red-orange crystals of the title compound **5** (0.41 g, 44% isolated yield). C₄₅H₉₆Li₃N₆Si₄: calcd. C 63.26, H 11.32, N 9.84; found C 62.08, H 10.96, N 10.21. ¹H NMR (400.23 MHz, [D₆]benzene, 294.3 K): δ = 0.00, 0.23, 0.39 (s, 27 H, 3 × SiMe₃), 1.4–2.4 (v. br., overlapping multiplet, 48 H, 3 × H_{tmEDA}), 3.03 (m, 2 H, 2 × *exo*-Me₃SiCHCH),

3.14 (m, 1 H, *endo*-PhSiCH, ³*J* = 24.0, ⁴*J* = 8.0 Hz, 1 H, 3.47, dd), 5.85 (m, 1 H, 6.39, m, 1 H), 6.70 (t, ³*J* = 28.0 Hz, *exo*-central allyl CHCHCH), 7.14–7.39 (br. overlapping multiplet, 5 H, SiPh protons), 7.89 (large, overlapping multiplets, 2 H) ppm. ¹³C NMR (100.65 MHz, [D₆]benzene, 295.8 K): δ = –3.7 (*endo*-SiMe₃), 0.0, 0.6 (2 × *exo*-SiMe₃), 44.0 (br., 4 × N(CH₃)₂), 55.1 (br., 2 × NCH₂CH₂N), 74.4 (*endo*-CHCHSiMe₃), 122.3, 124.6, 125.3 (C₆H₅Si), 133.3, 134.2, 151.2, 154.1 (2 × *exo*-CHCHSiMe₃) ppm. ⁷Li NMR (155.54 MHz, [D₆]benzene, 295.2 K): δ = 0.56, 0.79, 1.18 ppm.

[L²{Na(tmEDA)}₃] (6): A suspension of benzylna (0.17 g, 1.5 mmol) in hexane (20 mL) was cooled to –78 °C and tmEDA (0.18 g, 0.23 mL, 1.5 mmol) was added. The solution was stirred for 5 min and L²H₃ (0.223 g, 0.5 mmol) was added dropwise, then the reaction mixture was stirred at –78 °C for 30 min before being warmed to room temperature. Stirring for a further 48 h afforded a dark yellow solution and a precipitate, which re-dissolved on gentle heating. The resulting solution was filtered whilst hot (Celite, P3), and hexane (5 mL) was added. Storage of the solution at +5 °C for several days produced a crop of orange, plate-like crystals of **6**. C₇₂H₁₄₆N₈Na₆Si₈: calcd. C 58.17, H 9.90, N 7.54; found C 58.05, H 9.93, N 7.47. ¹H NMR (400.23 MHz, [D₆]benzene, 294.3 K): δ = –0.10, –0.06, 0.00, 0.12, 0.25, 0.32, 0.39, 0.41 (overlapping singlets, Si(CH₃)₃), 1.57–1.73 (br. m, allyl CH), 1.85 (br. s, tmEDA CH₂), 2.10 (br. s, tmEDA CH₃), 2.92–3.81 (br. overlapping m, allyl CH), 5.60–5.99, 6.14–6.42, 6.51–6.67 (br. overlapping m, allyl CH), 7.22–7.62 (br. overlapping m, 10 H, C₆H₅), 8.10–8.47 (allyl CH) ppm. ¹³C NMR (100.65 MHz, [D₆]benzene, 295.8 K): δ = –0.01, 1.01, 4.45, 4.60, 5.00, 5.21 [Si(CH₃)₃], 47.73 (tmEDA CH₃), 58.98 (tmEDA CH₂), 133.12, 134.93 (allyl CH-CH) ppm, resonances due to other allyl carbon atoms were too low in intensity to be distinguished from background noise.

[L¹{K(OEt)₂}₂KLi(μ -*OrBu*)₂] (7): *n*BuLi (1.6 mL, 1.91 mL, 3.1 mmol) was added dropwise to a mixture of L²H₃ (0.39 g, 1.0 mmol) and diethyl ether (10 mL) at –78 °C. After stirring for 30 min, the reaction mixture was warmed to room temperature,

and was stirred for a further 20 h. The resulting yellow solution was added to a solution of potassium *tert*-butoxide (0.35 g, 3.1 mmol) in diethyl ether (10 mL) to give an orange solution which was stirred for 4 h, filtered (Celite, P3) and concentrated to a volume of ca. 2 mL. Storage of the solution at -15°C overnight afforded orange crystals of the title compound **6**₂ (0.18 g, 35%). C₇₈H₁₇₆K₆Li₂O₁₀Si₈: calcd. C 53.61, H 10.15; found C 53.58, H 10.13. ¹H NMR (400.23 MHz, [D₆]benzene, 294.3 K): δ = 0.00–0.45 (br., overlapping multiplet, 30 H, 3 × SiMe₃, SiMe), 1.09 (Li-OrBu), 3.24 [2 × (CH₃CH₂)₂O], 6.07–6.34 (br., overlapping multiplet, 9 H, CHCHCH) ppm. ¹³C NMR (100.65 MHz, [D₆]benzene, 295.8 K): δ = –3.2 (SiMe), 0.0, 1.15, 4.8 (3 × SiMe₃), 17.4 (LiOrBu), 67.7, 69.8 [2 × (CH₃CH₂)₂O], 145.5, 147.9, 148.1 ppm, allyl carbon atoms.

[L¹{Li(pmdeta)}₃] (**8**): A mixture of L¹H₃ (0.38 g, 1.0 mmol) and hexane (20 mL) was cooled to -78°C and *n*BuLi (1.6 M, 1.9 mL, 3.0 mmol) was added dropwise. The reaction mixture was slowly warmed to room temperature and stirred for 4 h. Upon addition of pmdeta (0.64 mL, 3.0 mmol) a faintly turbid yellow solution was formed, which, on stirring overnight, became orange-red in colour. Filtration of the solution (Celite, P3) followed by concentration of the filtrate to ca. 2 mL and storage at -15°C for 2–3 d afforded orange crystals of **8** (0.36 g, 39%). C₄₆H₁₀₈Li₃N₉Si₄: calcd. C 60.02, H 11.82, N 13.69; found C 60.07, H 11.75, N 13.69. ¹H NMR (400.23 MHz, [D₆]benzene, 294.3 K): δ = 0.00, 0.14, 0.16, 0.23 (s, 30 H, 3 × SiMe₃, SiMe), 1.61, 1.64, 1.71, 1.80 (4 × dd, ³J = 7.78, ⁵J = 1.25 Hz, allyl CH-CH-CHSiMe and CH-CH-CHSiMe), 2.13 (s, 3.6 H, pmdeta N(CH₃)₂), 2.20 (s, 9 H, pmdeta NCH₃), 2.38 and 2.51 (t, ³J = 6.78 Hz, 24 H, pmdeta CH₂-CH₂), 5.46, 5.50, 5.60, 5.62, 5.65, 5.67, 5.71, 5.76 (overlapping m, allyl CH-CHSiMe), 6.08–6.24 (overlapping m, allyl CH-CHSiMe), 6.53, 6.58 (overlapping t, ³J = 7.78 Hz, allyl CH-CHSiMe), 7.09 (t, ³J = 15.81 Hz, allyl CH-CHSiMe *exo,exo*) ppm. ¹³C NMR (100.65 MHz, [D₆]benzene, 295.8 K): δ = –1.44, –0.34, 0.03, 3.18 (SiMe and 3 × SiMe₃), 25.67, 26.78, 29.29, 30.92 (terminal allyl carbon atoms), 43.69 (pmdeta NCH₃), 46.54 (pmdeta N(CH₃)₂), 57.45 and 58.87 (pmdeta CH₂), 124.98, 126.72, 130.01, 143.53, 144.13, 147.82 (central allyl carbon atoms) ppm. ⁷Li NMR (155.54 MHz, [D₆]benzene, 295.2 K): δ = –0.34, –0.17, 0.08 ppm.

Computational Details: All calculations are based on density functional theory (DFT) and were carried out using the Amsterdam Density Functional (ADF) program.^[43,44] Equilibrium geometries were fully optimized using analytical gradient techniques. The VWN functional of the local density approximation (LDA) was used,^[45] in combination with an uncontracted set of Slater-type orbitals (STOs). This basis set is designated DZP: it is of double- ζ quality and has been augmented with a set of polarization functions on each atom: 2p on H, 2p and 3d on Li, 3d on C, N and Si. The core shells of lithium (1s), carbon (1s), nitrogen (1s) and silicon (1s 2s 2p) were treated by the frozen-core approximation.^[43a] An auxiliary set of s, p, d, f and g STOs was used to fit the molecular density and to represent the Coulomb and exchange potentials accurately in each SCF cycle.^[43] Furthermore, the BP86 functional of the generalized gradient approximation (GGA) was used,^[46] in combination with the DZP basis set as well as the larger TZ2P basis set. The latter is of triple- ζ quality and has been augmented with two sets of polarization functions on each atom: 2p and 3d on H, 2p, 3d and 4f on Li, 3d and 4f on C, N and Si. Finally, environment effects were estimated by modeling solvation in water using the conductor-like screening model (COSMO).^[47] The same parameters were used as described in ref.^[47b]

Supporting Information (see also the footnote on the first page of this article): Figures of the computational structures of compounds

3 and **4**, with accompanying tables of selected bond lengths and angles.

Acknowledgments

We thank the following organisations for financial support: The University of Manchester, the Royal Society of Chemistry (RSC), the Netherlands Organization for Scientific Research (NWO-CW), the National Research School Combination – Catalysis of the Netherlands (NRSC-C); the Spanish Ministerio de Educación y Ciencia (MEC) (CTQ2008-03077/BQU), and DURSI of Generalitat de Catalunya (SGR2005-0238). The authors also thank Dr. S. M. Humphrey (University of Cambridge) for help with the solution for the crystal structure of compound **6**₂.

- [1] L. Chabaud, P. James, Y. Landais, *Eur. J. Org. Chem.* **2004**, 3173–3199.
- [2] Y. Yamamoto, N. Asao, *Chem. Rev.* **1993**, *93*, 2207–2293.
- [3] a) G. Wilke, M. Kröner, B. Bogdanović, *Angew. Chem.* **1961**, *73*, 755–756; b) G. Wilke, B. Bogdanović, P. Hardt, P. Heimbach, W. Keim, M. Kröner, W. Oberkirch, K. Tanaka, E. Steinrück, D. Walter, H. Zimmerman, *Angew. Chem. Int. Ed. Engl.* **1966**, *5*, 151–164.
- [4] K. H. Pannell, M. F. Lappert, K. Stanley, *J. Organomet. Chem.* **1976**, *112*, 37–48.
- [5] R. A. Layfield, S. M. Humphrey, *Angew. Chem. Int. Ed.* **2004**, *43*, 3067–3069.
- [6] R. A. Layfield, M. Buehl, J. M. Rawson, *Organometallics* **2006**, *25*, 3570–3575.
- [7] T. J. Woodman, Y. Sarazin, S. Garratt, G. Fink, M. Bochmann, *J. Mol. Catal. A* **2005**, *235*, 88–97.
- [8] M. Schormann, S. Garratt, M. Bochmann, *Organometallics* **2005**, *24*, 1718–1724.
- [9] B. Ray, G. Neyroud, M. Kapon, Y. Eichen, M. S. Eisen, *Organometallics* **2001**, *20*, 3044–3055.
- [10] C. K. Gren, T. P. Hanusa, A. L. Rheingold, *Organometallics* **2007**, *26*, 1643–1649.
- [11] K. T. Quisenberry, J. D. Smith, M. Voehler, D. F. Stec, T. P. Hanusa, W. W. Brennessel, *J. Am. Chem. Soc.* **2005**, *127*, 4376–4387.
- [12] J. D. Smith, T. P. Hanusa, V. G. Young Jr., *J. Am. Chem. Soc.* **2001**, *123*, 6455–6456.
- [13] T. J. Woodman, M. Schormann, D. L. Hughes, M. Bochmann, *Organometallics* **2004**, *23*, 2972–2979.
- [14] T. J. Woodman, M. Schormann, M. Bochmann, *Organometallics* **2003**, *22*, 2938–2943.
- [15] T. J. Woodman, M. Schormann, D. L. Hughes, M. Bochmann, *Organometallics* **2003**, *22*, 3028–3030.
- [16] R. E. White, T. P. Hanusa, B. E. Kucera, *J. Organomet. Chem.* **2007**, *692*, 3479–3485.
- [17] R. E. White, T. P. Hanusa, B. E. Kucera, C. N. Carlson, *J. Am. Chem. Soc.* **2006**, *128*, 9622–9623.
- [18] C. K. Simpson, R. E. White, C. N. Carlson, D. A. Wroblewski, C. J. Kuehl, T. A. Croce, I. M. Steele, B. L. Scott, V. G. Young Jr., T. P. Hanusa, A. P. Sattelberger, K. D. John, *Organometallics* **2005**, *24*, 3685–3691.
- [19] T. P. Hanusa, W. W. Brennessel, *J. Am. Chem. Soc.* **2004**, *126*, 10550–10551.
- [20] C. J. Kuehl, C. K. Simpson, K. D. John, A. P. Sattelberger, C. N. Carlson, T. P. Hanusa, *J. Organomet. Chem.* **2003**, *683*, 149–154.
- [21] R. A. Layfield, F. García, J. Hannauer, S. M. Humphrey, *Chem. Commun.* **2007**, 5081–5083.
- [22] C. K. Gren, T. P. Hanusa, W. W. Brennessel, *Polyhedron* **2006**, *25*, 286–292.
- [23] a) G. Fraenkel, A. Chow, W. R. Winchester, *J. Am. Chem. Soc.* **1990**, *112*, 1382–1386; b) G. Boche, G. Fraenkel, J. Cabral, K.

- Harms, N. J. R. van Eikema Hommes, J. Lohrenz, M. Marsch, P. v. R. Schleyer, *J. Am. Chem. Soc.* **1992**, *114*, 1562–1565.
- [24] G. Fraenkel, J. A. Cabral, *J. Am. Chem. Soc.* **1993**, *115*, 1551–1557.
- [25] G. Fraenkel, J. F. Qiu, *J. Am. Chem. Soc.* **1996**, *118*, 5828–5829.
- [26] G. Fraenkel, J. F. Qiu, *J. Am. Chem. Soc.* **1997**, *119*, 3571–3579.
- [27] G. Fraenkel, J. H. Duncan, J. Wang, *J. Am. Chem. Soc.* **1999**, *121*, 432–443.
- [28] P. B. Hitchcock, M. F. Lappert, W.-P. Leung, D.-S. Liu, T. C. W. Mak, Z.-X. Wang, *J. Chem. Soc., Dalton Trans.* **1999**, 1257–1262.
- [29] R. Fernández-Galán, P. B. Hitchcock, M. F. Lappert, A. Antiñolo, A. M. Rodríguez, *J. Chem. Soc., Dalton Trans.* **2000**, 1743–1749.
- [30] G. Fraenkel, A. Chow, R. Fleischer, H. Liu, *J. Am. Chem. Soc.* **2004**, *126*, 3983–3995.
- [31] C. Strohmann, H. Lehman, S. Dilsky, *J. Am. Chem. Soc.* **2006**, *128*, 8102–8103.
- [32] P. J. Bailey, S. T. Liddle, C. A. Morrison, S. Parsons, *Angew. Chem. Int. Ed.* **2001**, *40*, 4463–4466.
- [33] M. J. Harvey, T. P. Hanusa, V. G. Young Jr., *Angew. Chem. Int. Ed.* **1999**, *38*, 217–219.
- [34] K. T. Quisenberry, C. K. Gren, R. E. White, T. P. Hanusa, W. W. Brennessel, *Organometallics* **2007**, *26*, 4354–4356.
- [35] F. H. Allen, *Acta Crystallogr., Sect. B* **2002**, *58*, 380–388.
- [36] S. Corbelin, J. Kopf, N. P. Lorenzen, E. Weiss, *Angew. Chem. Int. Ed. Engl.* **1991**, *30*, 825–827.
- [37] a) J. C. Amicangelo, P. B. Armentrout, *J. Phys. Chem. A* **2000**, *104*, 11420–11432; b) D. Feller, D. A. Dixon, J. B. Nicholas, *J. Phys. Chem. A* **2000**, *104*, 11414–11419; c) T. B. McMahon, G. Ohanessian, *Chem. Eur. J.* **2000**, *6*, 2931–2941.
- [38] W. Clegg, A. M. Drummond, S. T. Liddle, R. E. Mulvey, A. Robertson, *Chem. Commun.* **1999**, 1569–1570.
- [39] J. F. Allan, R. Nassar, E. Specht, A. Beatty, N. Calin, K. W. Henderson, *J. Am. Chem. Soc.* **2004**, *126*, 484–485.
- [40] H. Köster, E. Weiss, *Chem. Ber.* **1982**, *115*, 3422–3426.
- [41] S. A. Solomon, C. A. Muryn, R. A. Layfield, *Chem. Commun.* **2008**, 3142–3144.
- [42] M. Schlosser, L. Franzini, *Synthesis* **1998**, 707–709.
- [43] a) G. te Velde, F. M. Bickelhaupt, E. J. Baerends, C. Fonseca Guerra, S. J. A. van Gisbergen, J. G. Snijders, T. Ziegler, *J. Comput. Chem.* **2001**, *22*, 931–967; b) F. M. Bickelhaupt, E. J. Baerends in: *Reviews in Computational Chemistry* (Eds.: K. B. Lipkowitz, D. B. Boyd); Wiley-VCH: New York, **2000**, Vol. 15, pp. 1–86; c) M. Swart, F. M. Bickelhaupt, *Int. J. Quantum Chem.* **2006**, *106*, 2536–2544.
- [44] Computer code ADF 2007.01: E. J. Baerends, J. Autschbach, A. Bérces, J. A. Berger, F. M. Bickelhaupt, C. Bo, P. L. de Boeij, P. M. Boerrigter, L. Cavallo, D. P. Chong, L. Deng, R. M. Dickson, D. E. Ellis, M. van Faassen, T. Fan, T. H. Fischer, C. Fonseca Guerra, S. J. A. van Gisbergen, J. A. Groeneveld, O. V. Gritsenko, M. Grüning, F. E. Harris, P. van den Hoek, C. R. Jacob, H. Jacobsen, L. Jensen, E. S. Kadantsev, G. van Kessel, R. Klooster, F. Kootstra, E. van Lenthe, D. A. McCormack, A. Michalak, J. Neugebauer, V. P. Nicu, V. P. Osinga, S. Patchkovskii, P. H. T. Philipsen, D. Post, C. C. Pye, W. Ravenek, P. Romaniello, P. Ros, P. R. T. Schipper, G. Schreckenbach, J. Snijders, M. Solà, M. Swart, D. Swerhone, G. te Velde, P. Vernooijs, L. Versluis, L. Visscher, O. Visser, F. Wang, T. A. Wesolowski, E. M. van Wezenbeek, G. Wiesenekker, S. K. Wolff, T. K. Woo, A. L. Yakovlev, T. Ziegler, SCM, Amsterdam, The Netherlands.
- [45] S. H. Vosko, L. Wilk, M. Nusair, *Can. J. Phys.* **1980**, *58*, 1200–1211.
- [46] a) J. P. Perdew, *Phys. Rev. B* **1986**, *33*, 8822–8824 (Erratum: *ibid.*, 8834, 7406); b) A. D. Becke, *Phys. Rev. A* **1988**, *38*, 3098–3100.
- [47] a) A. Klamt, G. Schüürmann, *J. Chem. Soc., Perkin Trans. 2* **1993**, 799–805; b) A. Klamt, *J. Phys. Chem.* **1995**, *99*, 2224–2235; c) M. Swart, E. Rösler, F. M. Bickelhaupt, *Eur. J. Inorg. Chem.* **2007**, 3646–3654.

Received: July 1, 2009
Published Online: August 6, 2009